RGNZ/MGPB

Rudarsko-geološko-naftni zbornik
(The Mining-Geology-Petroleum Engineering Bulletin)
DOI: 10.17794/rgn.2025.4.3

Original scientific paper

Rock Magnetism and Geochemistry Analyses of Surface Sediments at Maar Lake: Study Case at Ranu Klakah, East Java, Indonesia

Fathia Matondang[1], Satria Bijaksana[1]*, Ulvienin Harlianti[1], Ni Komang Tri Suandayani[2], Yohansli Noya[1], Putu Billy Suryanata[1], Khalil Ibrahim[1], Thomas Andre Maris Widagdo[1], Mamilla Venkateshwarlu[3,4], Animireddi Venkata Satyakumar[3,4]

[1] *Faculty of Mining and Petroleum Engineering, Institut Teknologi Bandung, Jalan Ganesa 10, Bandung 40132, Indonesia.*
[2] *Faculty of Mathematics and Natural Sciences, Universitas Udayana, Badung, Bali, Indonesia.*
[3] *CSIR-National Geophysical Research Institute (CSIR-NGRI), Hyderabad, India.*
[4] *Academy of Scientific and Innovative Research (AcSIR), Ghaziabad, India.*

Abstract

Ranu Klakah is a maar lake that is part of the Lamongan Monogenetic Volcanic Field (LMVF), East Java, Indonesia, which has a closed hydrological system. This study aims to understand the characteristics of Ranu Klakah surface sediments through rock magnetism and geochemical analyses. Tests were conducted on 16 sample points derived from surface sediments in the lake and springs around the lake. The results of rock magnetism analysis in Ranu Klakah surface sediments showed the presence of magnetite and titanomagnetite minerals. This is supported by XRD (X-Ray Diffraction) analysis, where the minerals magnetite, albite, and illite were found in sediments from inside the lake and springs around the lake. From the combined results of these two methods, it was concluded that the surface sediments in Ranu Klakah have pseudo-single-domain magnetite minerals type that originated from the weathering of rocks around the lake and there has been no diagenesis of the surface sediments in the lake due to the absence of results showing mineral changes in the samples tested.

Keywords:
Maar Lake, Lamongan Monogenetic Volcanic Field, rock magnetism, geochemistry, East Java

1. Introduction

Maars are a type of volcanic landscape formed from phreatomagmatic eruptions, which are explosive events triggered when magma interacts with shallow groundwater. This process produces ash-rich and highly explosive eruptions (**Lorenz, 1986; Graettinger, 2018; and Gurusinga et al., 2023**). Clusters or fields of multiple craters often contain maars, where eruptions occur in close succession within a specific time frame (**Lorenz, 1986; Volosín and Risso, 2019**). This phenomenon makes maar lakes important geological features to study, particularly in relation to the evolution of local volcanism and sediment formation processes.

One intriguing example of a maar lake is Ranu Klakah ("Ranu" is the name for the lake in East Java, Ranu Klakah has the same meaning as Lake Klakah), located in the Lamongan Volcanic Complex, East Java, Indonesia. The Lamongan Volcano is recognised as Indonesia's only monogenetic volcanic field, also known as Lamongan Monogenetic Volcanic Field (LMVF). This region formed through a series of small-scale volcanic activities with relatively short eruption periods, producing scattered volcanic craters throughout the area (**Gurusinga et al., 2023**). This uniqueness makes Ranu Klakah an important site for research, particularly for understanding the interactions between volcanic activity, sediment dynamics, and the influence of human activities on the surrounding environment. Lake sediments are considered "natural archives" that record valuable information about environmental conditions (**Yunginger et al., 2018; Suandayani et al., 2023; Fu et al., 2024; Tekin-Özan et al., 2024**). Factors such as geological processes, rock weathering, water cycles, volcanic activity, and anthropogenic influences are the primary determinants of lake sediment composition (**Wang et al., 2017; Asaah et al., 2020; Tao et al., 2021; Sabatier et al., 2022**).

This maar lake with a diameter of 675 metres, has a closed hydrological system, with no river inflow into the lake. The water source comes from several springs around the lake, protecting it from external influences.

* Corresponding author: Satria Bijaksana
e-mail address: satria@itb.ac.id
Received: 21 November 2024. Accepted: 21 February 2025.
Available online: 27 August 2025

This condition allows the surface sediments of the lake to be attributed mainly to the weathering of surrounding volcanic rocks (**Fagel et al., 2024**). The ecosystem of Ranu Klakah is not only shaped by natural processes. Human activities, such as the use of floating net cages for fish farming and the presence of small food stalls around the lake, also contribute to the dynamics of the lake's environment. The interaction between anthropogenic activities and natural processes is an important factor that needs further study, especially regarding its impact on water quality, mineral content, and sediment ecosystems (**Barut et al., 2018**).

This study aims to assess the characteristics of surface sediments in Ranu Klakah using rock magnetism and geochemical methods. This research is important because the analysis of surface sediments using rock magnetism and geochemical methods in maar lakes is still rarely done, especially in Indonesia. It aims to analyse the influence of volcanic rock weathering and human activities on the lake environment. We try to gain deeper insight into how geological and anthropogenic factors collectively influence environmental change, especially in unique volcanic areas such as LMVF, through this study.

2. Materials and Methods

Administratively, Ranu Klakah is located in Lumajang Regency, East Java Province, Indonesia. This study began with bathymetric measurements using a Garmin Striker Plus 7SV APAC device, revealing that the lake has a depth of up to 28 metres. Field activities were conducted in July 2024. This was followed by sampling Ranu Klakah's surface sediments using a sediment grabber deployed from a boat, as well as soil samples from around the lake, obtained by exploring spring areas near the lake. Twelve surface sediment samples from within the lake and four soil samples from nearby springs were collected (see **Figure 1**). To avoid reactions between elements or minerals with oxygen in the sediment, 10 mL of HNO_3 is added to every 5 L of sediment (**Siaka et al., 1998**). The surface sediment samples were sorted with a 325-mesh sieve (44 μm diameter) to produce uniform clay particles. The sieved samples were dried and then prepared for magnetic analysis. Sample preparation and magnetic parameter measurements were carried out according to the method described in detail by **Yunginger et al. (2018)**. The dried samples were placed in cylindrical plastic containers with a diameter of 2.5 cm and height of 2.2 cm (volume of 10 cm^3). Some samples were extracted using a magnetic stirrer IKA Lab-Disc 3907500 to separate the magnetic minerals and selected for testing the physical properties of magnetic minerals.

To obtain magnetisation parameters, rock magnetism experiments conducted include the measurement of magnetic susceptibility (χ), hysteresis curve, isothermal remanent magnetisation (IRM), and thermomagnetic curves. Sixteen samples were tested for magnetic susceptibility, consisting of twelve surface sediment samples from the lake and four soil samples from springs around the lake. This study employed a Bartington MS3 magnetic susceptibility system (Bartington Instruments Ltd., Witney, UK) to determine the mass-specific magnetic susceptibility at low frequency (χ_{LF}) and high frequency (χ_{HF}). Measurements were conducted using a dual-frequency MS2B sensor operating at 0.47 KHz for low frequency (LF) and 4.7 KHz for high frequency (HF). The frequency-dependent magnetic susceptibility (χ_{FD}%) was calculated using the equation $\chi_{FD}\% = 100\% (\chi_{LF} - \chi_{HF})/\chi_{LF}$ (**Dearing, 1994**). The magnetic measurements were performed at the Rock Physical Properties Characterization and Modeling Laboratory, Faculty of Mining and Petroleum Engineering (FTTM), Institut Teknologi Bandung (ITB), Indonesia. The χ_{LF} parameter is often used as a proxy indicator for the concentration of magnetic minerals, primarily ferromagnetic phases such as magnetite and hematite (**Yunginger et al., 2018; Fajar et al., 2022; Suandayani et al., 2023**). We used the Advanced Variable Field Translation Balance (AVFTB) to test five extracted samples of surface sediment at CSIR-National Geophysical Research Institute (CSIR-NGRI) in Hyderabad, India, for hysteresis loops, IRM, and thermomagnetic (χ-T curves). The magnetic field applied to the test is up to 1 T and temperatures are up to 700°C. We applied the HystLab software (**Paterson et al., 2018**), to correct the paramagnetic hysteresis curves. From these curves, we derived hysteresis parameters, including coercivity (B_c), remanent coercivity (B_{cr}), saturation magnetisation (M_s), and saturation remanent magnetisation (M_{rs}). Using these parameters, we constructed a Day plot from (**Dunlop, 2002**) to assess the magnetic mineral domain states. Magnetic domains play a critical role in shaping the coercivity spectrum of individual minerals (**Bijaksana et al., 2022**).

All samples were subjected to geochemical analysis using the Rigaku Supermini200 benchtop WDXRF (wavelength dispersive X-ray fluorescence) spectrometer system (Rigaku Corp., Tokyo, Japan), to identify the major elements present in the sediment samples. Statistical analyses were conducted in Origin 2023b, including principal component analysis (PCA) calculations, and hierarchical cluster analysis (HCA). The clusters were determined by selecting an 80% similarity cut-off level in the dendrogram. This threshold was chosen to provide more detailed insight into the variables' relationships, resulting in three primary clusters. These statistical approaches were used to evaluate potential sources and relationships among elements present in surface sediments in the study area and to determine their sources. The suitability of the numbers for PCA analysis was previously thoroughly confirmed through Bartlett's test of sphericity, which helps to clarify whether the data set for the subject is suitable for analysis, or to check the assumption

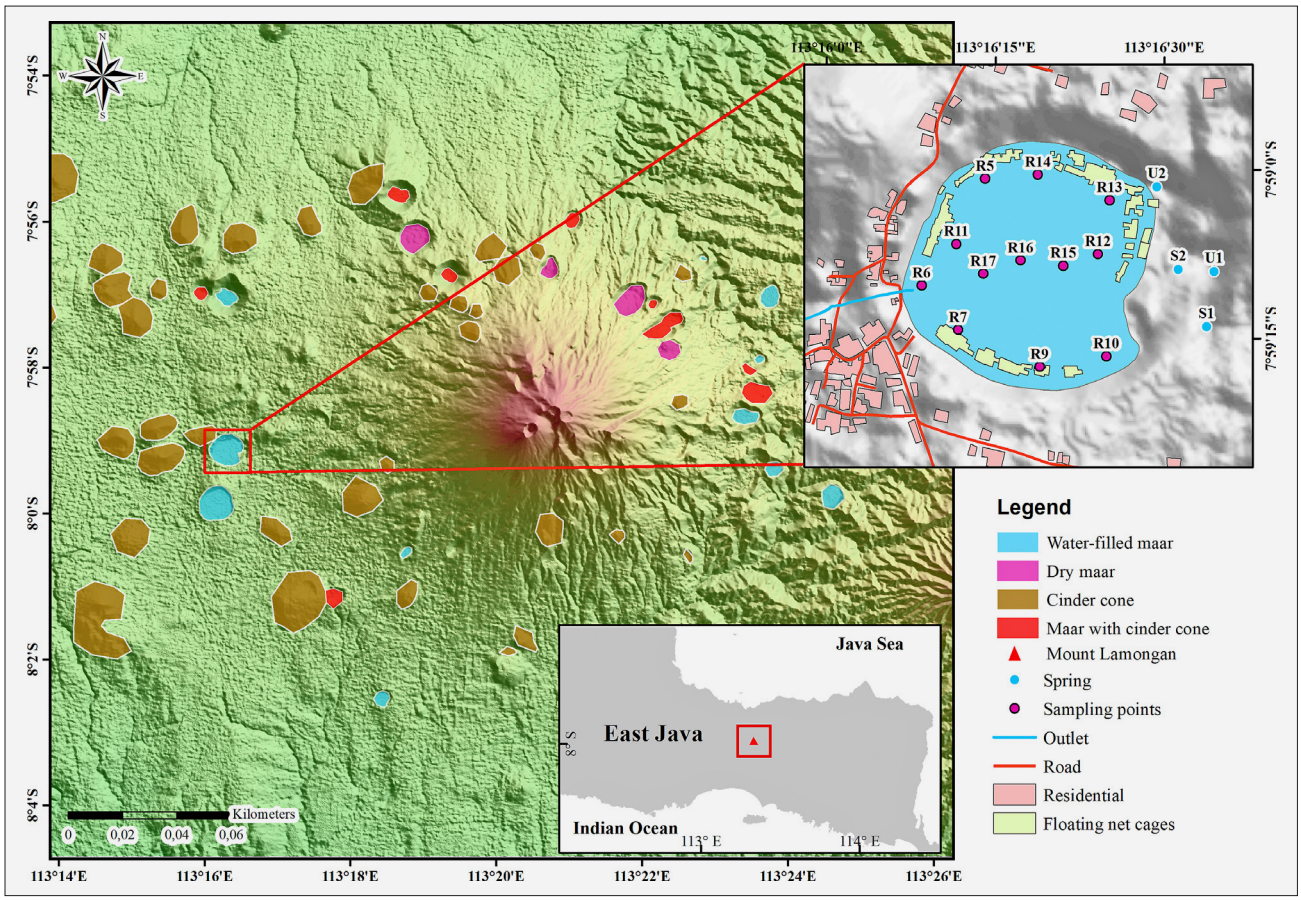

Figure 1. Map of research location at Ranu Klakah modified from **Carn (2000)** and **Gurusinga et al. (2023)**. Samples with an R code represent Ranu, which means the sample is inside the lake; the U and S codes represent that the sample comes from the spring around the lake (U located in the north and S located in the south).

that the population variances in a correlation or covariance matrix are equal (**Noya et al., 2024; Topaldemir et al., 2023; Yuksel et al., 2022**). Additionally, mineralogical composition of sediment-extracted samples was analysed using a Rigaku Smartlab XRD (X-Ray Diffraction) system (Rigaku Corp., Tokyo, Japan) with a Cu–K_α radiation source (λ=1.54 Å). The diffractometer operated at 40 kV and 30 mA with 2θ angles varying from 15° to 65° in continuous scanning mode. The diffracted beam was measured using a Kβ filter that effectively eliminates Kβ interference and ensures that only higher-angle diffraction lines were used for subsequent peak analysis (**Krishna et al., 2017**). The XRF and XRD analyses were conducted at the Hydrogeology and Hydrogeochemistry Laboratory, FTTM, ITB.

3. Results

3.1. Magnetic Properties

The magnetic susceptibility (χ) values of the 12 surface sediment samples in Ranu Klakah show a range of 316.74 to 953.76 x 10^{-8} m^3/kg, as illustrated on the distribution map of magnetic susceptibility (χ) values in **Figure 2**. The magnetic susceptibility (χ) values were larger in the area close to the spring (east side) and had smaller values around the lake outlet (west side). There is a direct correlation between ferromagnetic mineral concentrations and magnetic susceptibility values; higher mineral concentrations result in greater susceptibility values and vice versa.

Loop hysteresis is used to determine the magnetic particle size of the sample. Hysteresis loop, IRM, and thermomagnetic tests were conducted on three representative samples representing each class of magnetic susceptibility values. The samples consist of the highest value (R13), medium value (R6), and lowest value (R16), as well as two samples from springs around the lake (U1 and U2), which had higher magnetic susceptibility values among the three sample points from the lake. The hysteresis curves show that all five samples are well-saturated (see **Figure 3a-e**). All samples started to saturate when the magnetic field was 440 mT and the loops were completely closed at 800 mT. The smooth and slender shape of the hysteresis loop indicates that the magnetic minerals are dominated by pseudo-single-domain (PSD) or particles with a combination of single and multi-domain (SD + MD) (**Fu et al., 2024**).

The hysteresis curves, corrected for the paramagnetic component, are then plotted using Day plots (see **Figure**

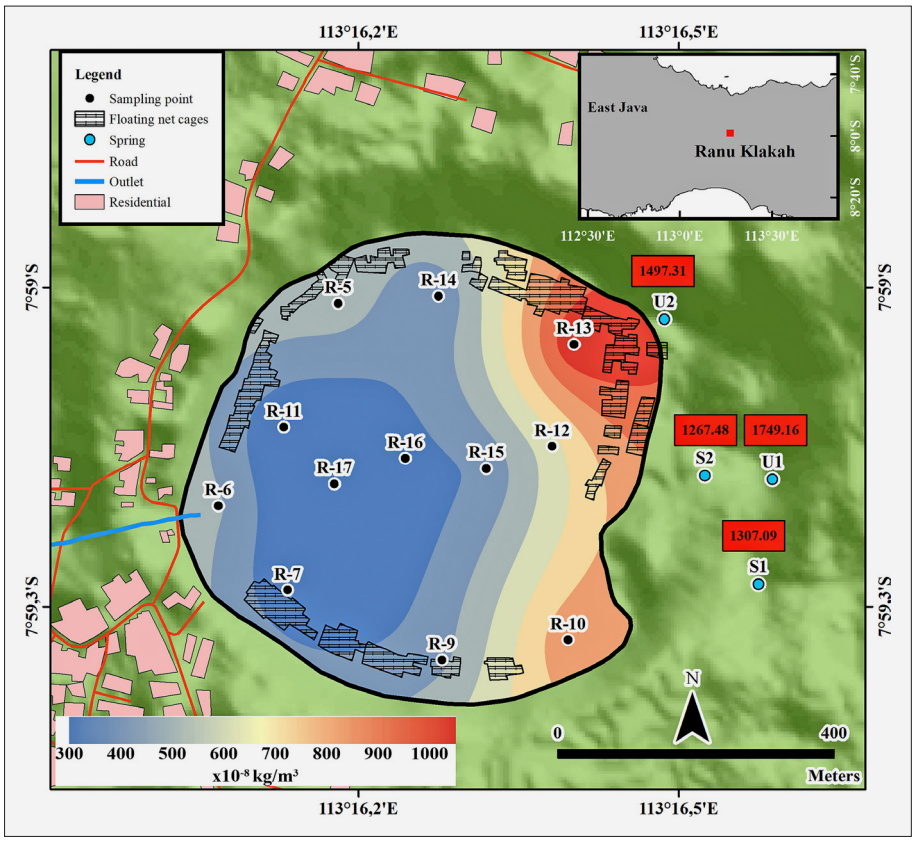

Figure 2. Spatial distribution of magnetic susceptibility values of Ranu Klakah surface sediments

4a) and Néel diagrams or squareness plots (see **Figure 4b**) to identify the domain nature of magnetic mineral. In the Day plot, the hysteresis parameter displayed is the ratio between M_{rs} and M_s versus the ratio between B_{Cr} and B_c (**Day et al., 1977**). The results showed that all samples were falling in the PSD area. To strengthen the analysis of the domain state on the Day plot, an analysis was also performed using the Néel plot (see **Figure 4b**), where the hysteresis parameter displayed is M_r/M_s vs. B_c (**Tauxe et al., 2002**). The M_r/M_s values on the Néel plot show 0.15-0.2 and B_c 10.8-15.6 mT, thus placing all sediment samples in the boundary area for the uniaxial single domain and superparamagnetic grains (USD+SP). They are not exactly on the pure magnetite line (black dashed line) nor the pure titanomagnetite line TM 60 (grey dashed line). This indicates the substitution of titanium (Ti) to the magnetite mineral in the sample (**Vigliotti et al., 2022**). In all samples, the IRM curves reach saturation when the applied field is between 300-400 mT, and from the backfield demagnetisation curves, the B_{cr} value is approximately 40 mT (see **Figure 5**). This suggests that all samples contain magnetite or titanomagnetite minerals (**Sudarningsih et al., 2017; Fu et al., 2024; Venkateshwarlu and Satyakumar, 2024**).

Thermomagnetic curves contain Curié temperature (Tc) information which is used to identify mineral types because each mineral has a different Curié temperature. All samples tested showed the same pattern of reversible behaviour (see **Figure 6a-e**). Samples from both the lake and the spring have similar Tc values, which are between 550°C and 580°C. From the thermomagnetic curve, the mineral that has a Curié temperature in that range is magnetite or titanomagnetite (**Venkateshwarlu and Satyakumar, 2024**).

3.2. Geochemistry and Mineral Analysis

X-Ray Fluorescence (XRF) analysis was performed to determine the composition and concentration of elements present in the sample. The two elements that had the highest values were Si at 24.22 – 35.53 mass% and Fe at 3.8 – 9.93 mass%. Heavy metal elements such as Hg, Pb, Co, and Zn were not detected in the samples tested. The elemental values are shown in **Table 1**. XRD analysis aimed to show the presence of several types of minerals in the samples. XRD analysis was carried out on five extracted samples, similar to the five extracted-samples used in the magnetic properties analysis. Representative samples are shown in **Figure 7a-b**. Both the samples contained minerals magnetite, albite, and illite.

4. Discussion

Klakah Lake has a closed system, where the lake does not have a river as an inflow that enters the lake, but has an outlet that exits (near the R6 sample point). Water from inside the lake comes only from springs around the lake, rain, and surface water. Therefore, the surface deposits in the lake come from the weathering of rocks that occur around the lake, and the diagenesis process has not

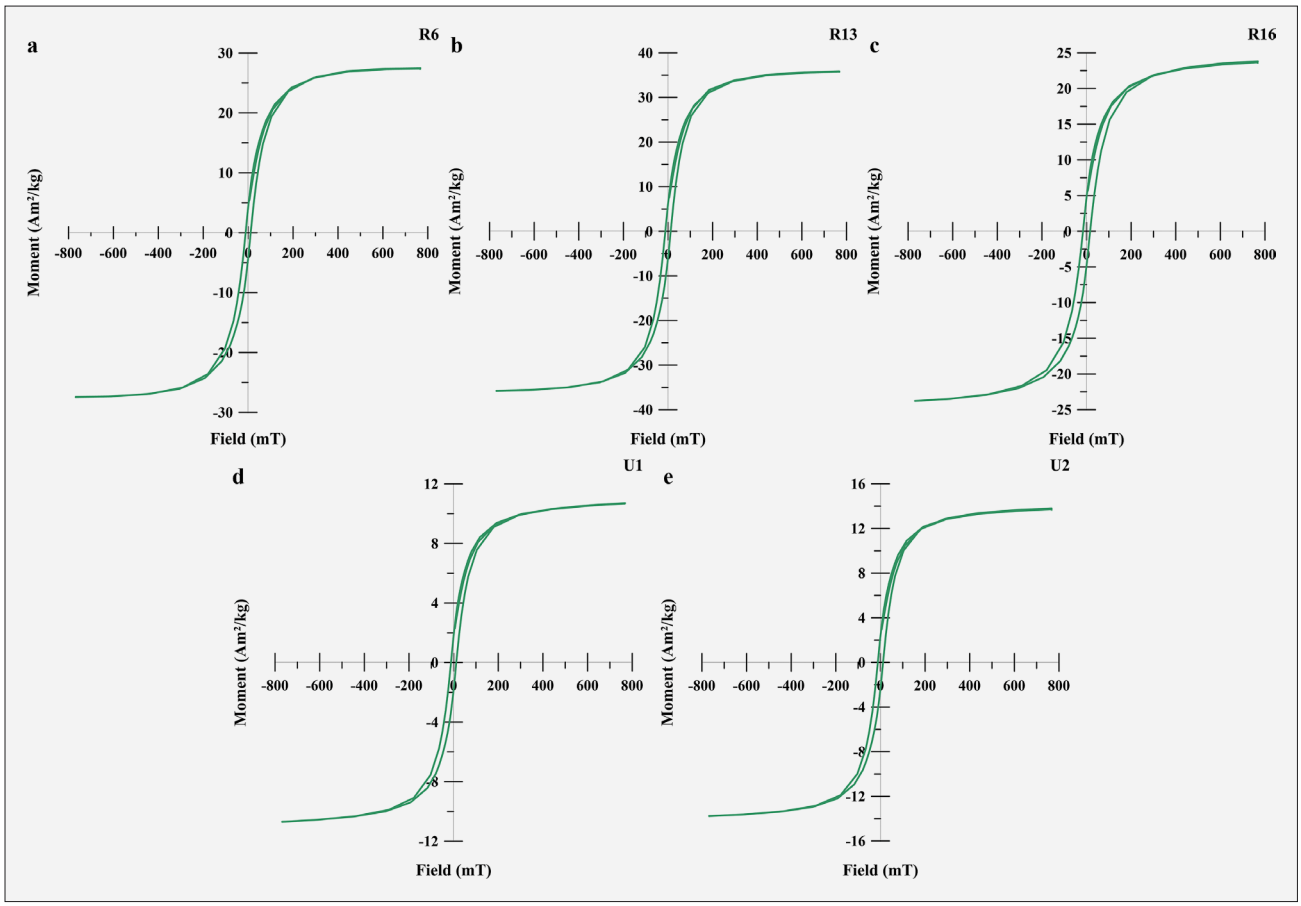

Figure 3. Hysteresis curves from testing samples of lake surface sediment in Ranu Klakah.
a) sample R6; b) sample R13; c) sample R16; d) sample U1; e) sample U2.

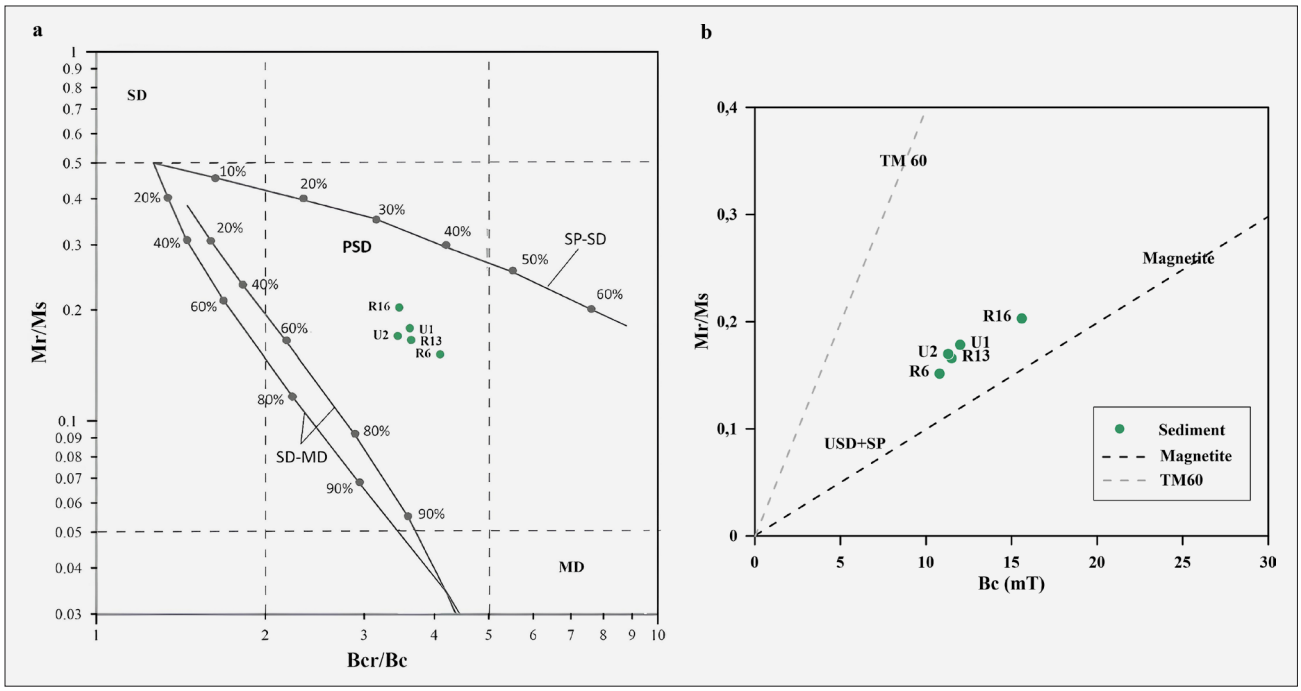

Figure 4. a) Day plot for five surface sediments representing different magnetic susceptibility values (**Day et al., 1977**)
b) Néel plot as squareness (M_{rs}/M_s) vs coercivity (B_c). The grey dash line shows trends for TM60 for pure titanomagnetite and bold dash line for pure magnetite (**Tauxe et al., 2002**).

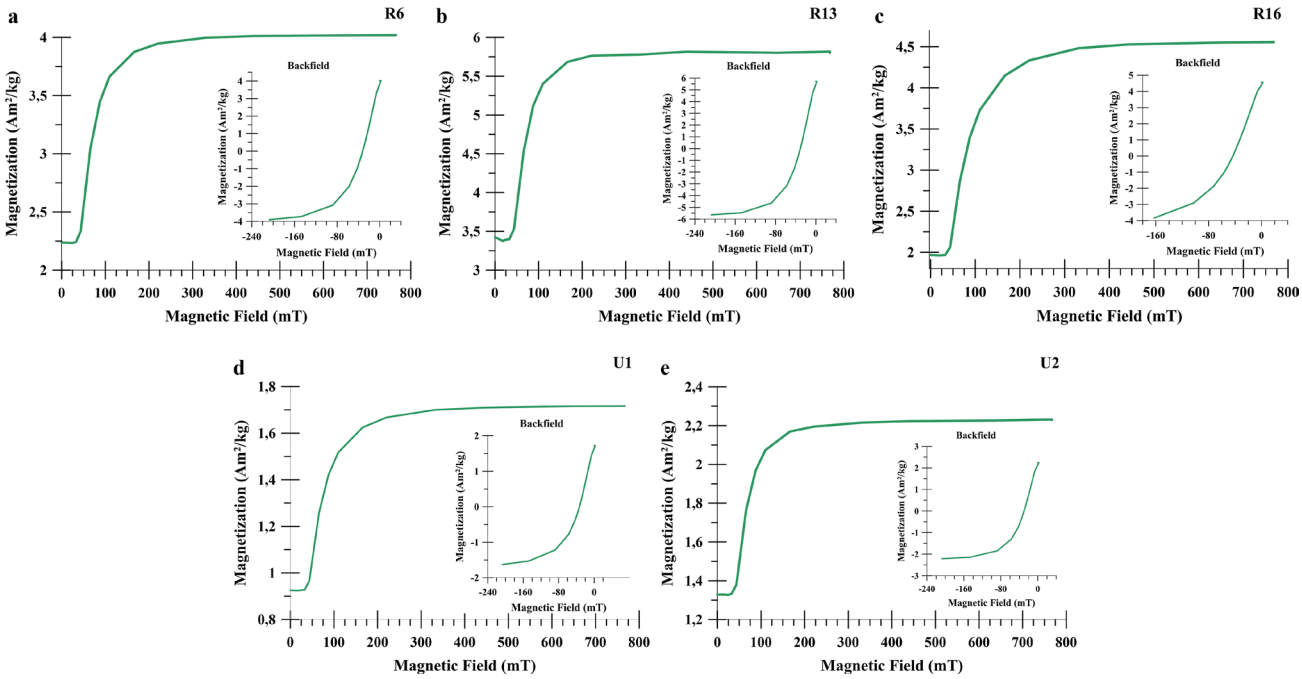

Figure 5. Isothermal remanent magnetization (IRM) of selected samples with insert the coercivity responses of the samples. a) sample R6; b) sample R13; c) sample R16; d) sample U1; e) sample U2.

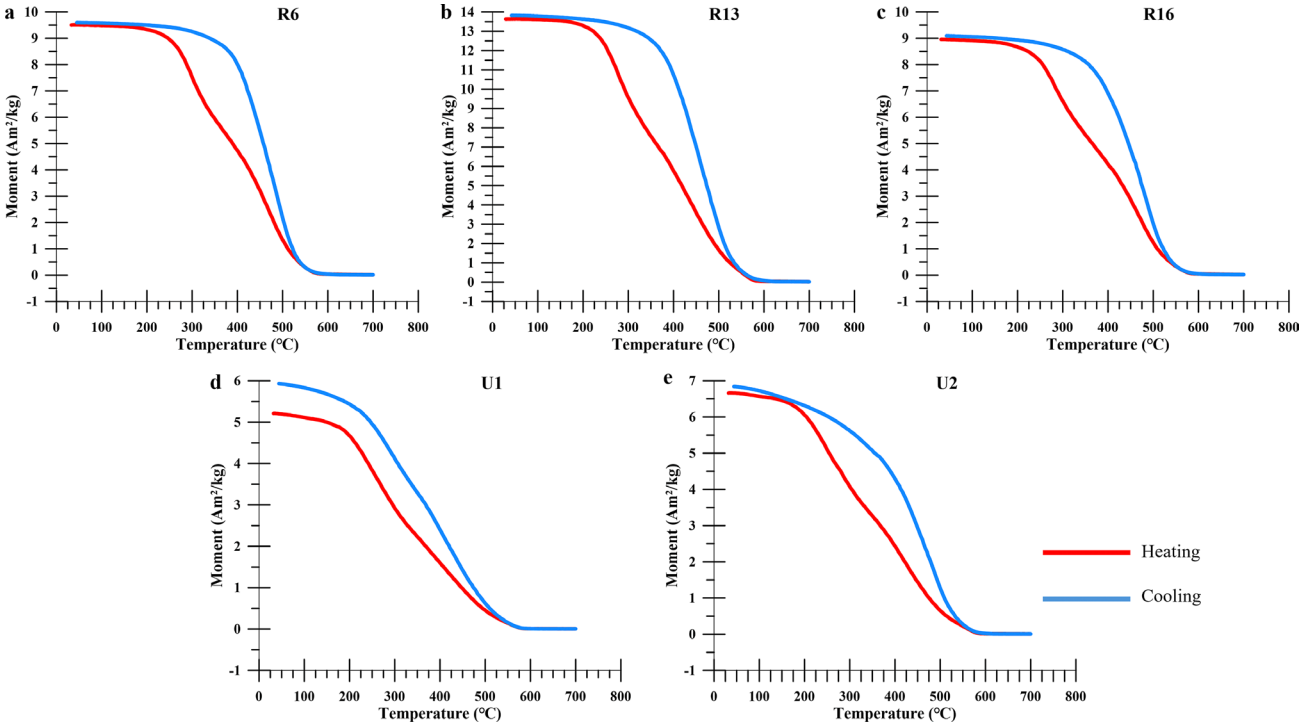

Figure 6. Thermomagnetic curves (χ-T) of surface sediments and rock samples. Red lines indicate heating curves, and blue lines indicate cooling curves a) sample R6; b) sample R13; c) sample R16; d) sample U1; e) sample U2.

occurred in the lake sediments. **Figure 2** shows the magnetic susceptibility values in the lake vary, where the highest values are on the east side (R13 and R10), medium on the west side (R6–near outlet), and the lowest in the centre of the lake (R-17). The sample point with the highest value for surface sediment samples from the lake was close to the spring source. The four soils originating from the spring source had higher magnetic susceptibility values than all sediment samples from the lake. The results of the hysteresis curve that has been corrected paramagnetically and then plotted into the Day plot and Néel Diagram (see **Figure 4a-b**), show that all samples

Table 1. Results of XRF analysis (mass%)

Sampling point	Element (mass%)													
	Na	Mg	Al	Si	P	S	Cl	K	Ca	Ti	Mn	Fe	Cu	Sr
U1	0.59	0.55	11.43	25.76	0.21	0.34	0.02	0.70	0.61	0.75	0.07	7.97	0.02	0.05
U2	0.49	0.46	12.23	26.27	0.17	0.16	0.10	0.54	0.47	0.67	0.05	8.18	0.02	0.04
S1	0.55	0.60	12.33	24.22	0.41	0.15	0.01	0.56	0.48	0.72	0.32	9.93	0.02	0.05
S2	0.52	0.43	12.12	25.90	0.28	0.22	0.04	0.59	0.50	0.61	0.06	8.60	0.02	0.04
R5	0.15	0.24	6.67	30.53	0.18	1.73	0.11	0.34	5.78	0.31	0.13	5.15	0.02	0.02
R6	0.16	0.19	5.02	33.38	0.12	1.44	0.04	0.26	5.30	0.24	0.06	4.43	ND	0.02
R7	0.13	0.16	4.06	35.48	0.13	1.47	0.10	0.31	4.02	0.21	0.03	3.81	ND	0.02
R9	0.26	0.19	5.51	33.43	0.12	1.56	0.06	0.30	4.22	0.29	ND	4.47	0.01	0.02
R10	0.32	0.36	7.46	32.21	0.15	0.96	0.27	0.35	2.22	0.38	0.08	6.05	0.01	0.02
R11	0.19	0.22	4.54	34.41	0.14	1.54	0.07	0.37	4.31	0.19	0.04	4.14	0.01	0.02
R12	0.35	0.33	6.46	32.68	0.13	1.35	0.04	0.32	2.98	0.38	0.05	5.46	0.01	0.02
R13	0.42	0.48	9.85	29.17	0.20	0.85	0.03	0.42	2.73	0.41	0.07	6.92	0.02	0.03
R14	0.17	0.23	4.94	34.17	0.14	1.46	0.29	0.35	3.85	0.27	0.04	4.39	0.01	0.02
R15	0.24	0.27	5.07	33.15	0.15	1.94	0.32	0.28	3.95	0.25	0.03	4.80	0.01	0.02
R16	0.31	0.22	4.61	34.97	0.13	1.48	0.08	0.30	3.47	0.21	0.04	4.18	ND	0.01
R17	0.22	0.13	4.10	35.53	0.13	1.52	ND	4.22	3.63	0.17	0.06	4.06	0.01	0.01
Max	0.59	0.60	12.33	35.53	0.41	1.94	0.32	4.22	5.78	0.75	0.32	9.93	0.02	0.05
Ave	0.32	0.32	7.28	31.33	0.17	1.14	0.11	0.64	3.03	0.38	0.07	5.78	0.02	0.03
Min	0.13	0.13	4.06	24.22	0.12	0.15	0.01	0.26	0.47	0.17	0.03	3.81	0.01	0.01

Note: ND means Not Detectable

have uniform magnetic mineral content and domains. This applies to samples from lakes and springs. The results of the IRM analysis and thermomagnetic curves also show that the minerals contained in all samples are magnetite and titanomagnetite. In the cooling curve, the magnetic value does not exactly return to the point before heating (especially for sample U1–**Figure 6d**). This is because the heating process of the sample was carried out at room temperature, which allowed the sample to oxidise and reduce its magnetic properties, but this was not a significant problem. From the results of the hysteresis curve, IRM, and thermomagnetic curve, similar results were obtained for all samples tested, indicating that the variation in magnetic susceptibility values only varies with the amount of mineral, not the type of mineral. This is confirmed by previous research by **Tamuntuan (2010)** at Lake Bedali and Lake Lading (lakes adjacent to Lake Klakah), both have a pseudo-single-domain magnetite mineral type, originating from the surrounding crater.

The XRF results were then subjected to HCA and PCA, which are used to determine the source of elements contained in sediment (**Noya et.al., 2024**). HCA displayed on the dendrogram shows the relationship between chemical elements in Ranu Klakah sediments based on their similarity (see **Figure 8**). This analysis identified several clusters of elements with different distribution patterns and geochemical origins. Na, Mg, Al, Fe, Ti, and Sr formed one cluster with a high degree of similarity, indicating the dominance of primary volcanic materials, such as plagioclase and pyroxene (**Vogel et al., 2017**). The minerals identified through XRD analysis show the content of elements belonging to this cluster. Clusters of Si, S, Ca, Cl, and K indicate the influence of chemical weathering or lake-water interaction with volcanic materials. P, Mn, and Cu are separated into different clusters. P and Mn reflect organic matter contributions, which may be related to fish farm activities (**Storebakken et al., 1998; Kaushik et al., 2004; Varol, 2019**), and derived from pesticides in agricultural activities for Cu (**Panagos et al., 2018**). The interconnected presence of Cl and S indicated possible traces of hydrothermal activity. Overall, this cluster pattern reveals the combined influence of volcanic geological factors and human activities in shaping the sediment composition of Ranu Klakah. The clusters in this dendrogram can be a reference in separating which elements are sourced from volcanic geology, such as Fe, Mg, and Ti, and those caused by human activities, such as P and Mn.

PCA (see **Figure 9a-b**) revealed three principal components with eigenvalues greater than 1, which accounted for 93.22% of the total variance. Therefore, the com-

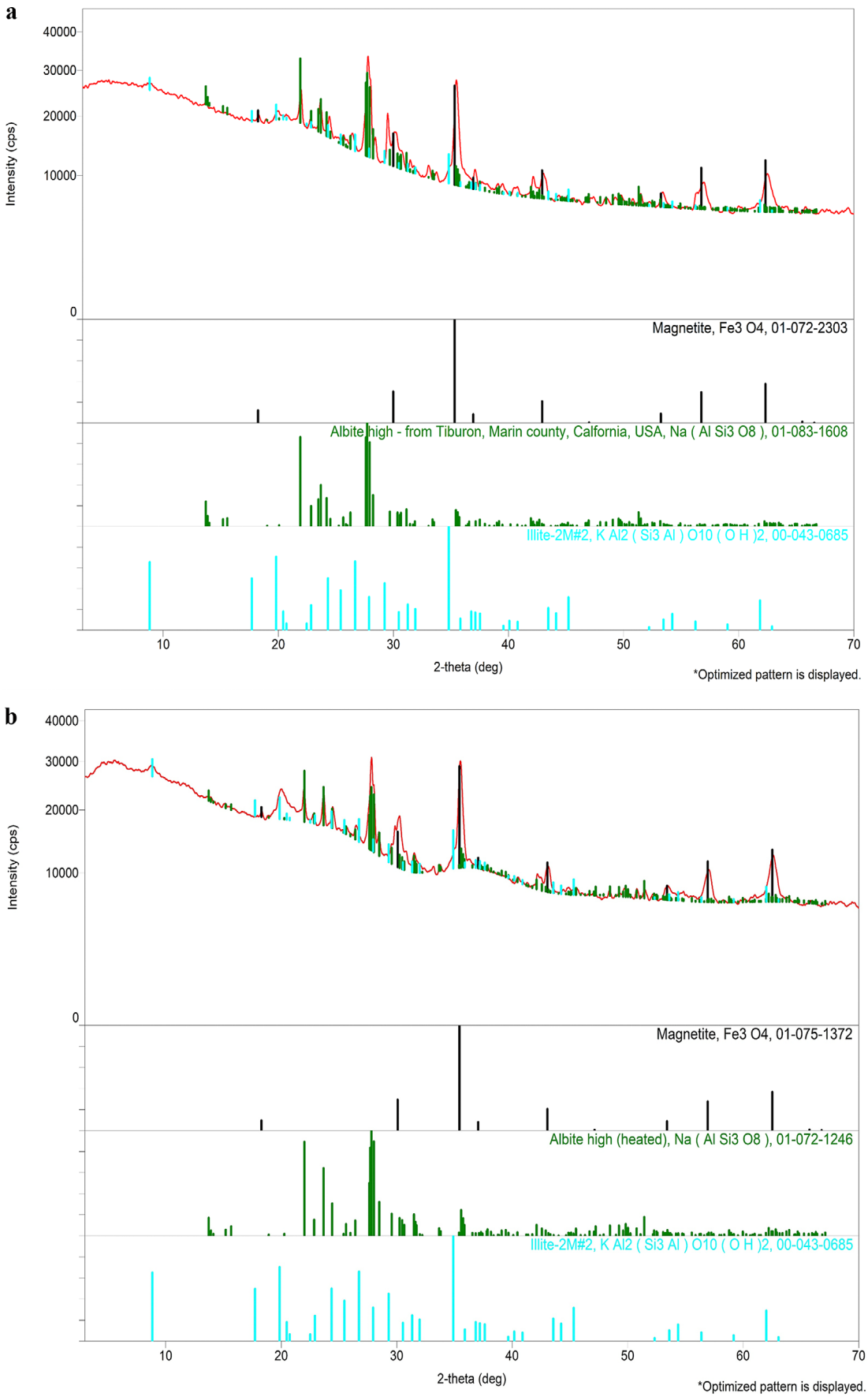

Figure 7. XRD measurement results for study at Ranu Klakah: a) R6 (representative sample from lake – near outlet); b) U2 (representative sample from spring).

ponent plot in rotated space shows that the elements in the sediment specimen are related to three different sources. Factor 1 (77.67%) is lithogenic or geological for Cl, Si, S, and Ca, factor 2 (10.05%) is lithological and anthropogenic for Na, Mg, Al, K, Ti, Fe, Cu, and Sr, and factor 3 (5.48%) is anthropogenic for Mn and P. The elements from factor 1 (Cl, Si, S, and Ca) are closely related to natural geological processes, such as weathering of volcanic rocks, sediment transport, and mineral deposition, reflecting the strong influence of the monogenetic volcanic environment in which the lake is located. The dominance of Cl, Si, S, and Ca indicates that the sediments were mainly derived from volcanic ash, tuff, and weathering of Si and Ca-rich volcanic rocks. Although lake water activities may slightly influence the presence of Cl, the main contribution of this element still comes from lithogenic sources. Thus, the sediments in Ranu Klakah largely reflect geological material from local volcanic activity.

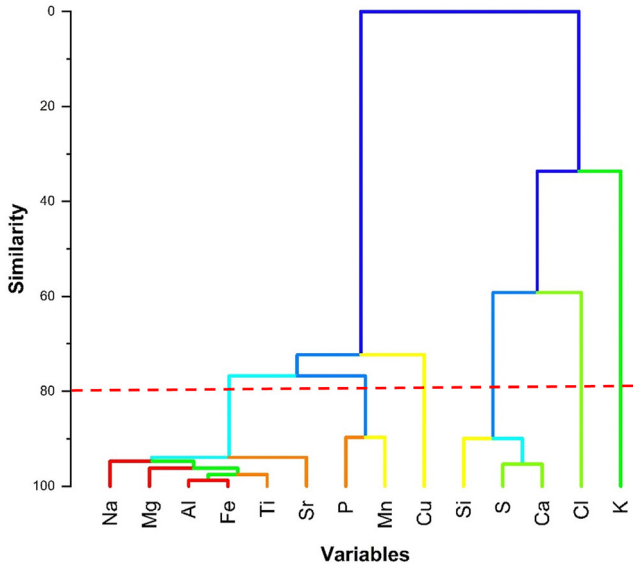

Figure 8. Dendrogram of HCA of surface sediment of Ranu Klakah with 80% similarity cut-off level

The second factor influencing sediments in Ranu Klakah is a combination of lithology and anthropogenic activities, characterised by the presence of major elements Na, Mg, Al, K, Ti, Fe, Cu, and Sr. These elements reflect the influence of minerals from volcanic rocks, such as feldspar, mica, and iron-titanium minerals (titanomagnetite), indicating lithological contributions through erosion and weathering of host rocks around the lake. In addition, Cu and Sr are important indicators of human activity (anthropogenic), where Cu may originate from lake waste, fish feed, or pesticide use, while Sr is associated with phosphate-containing fish feed residues, commonly used as a nutrient source for fish growth. The elements Na and Cu also show the influence of fish farming activities around the lake. Thus, Ranu Klakah sediments are influenced by the interaction between local lithological processes and surrounding human activities.

The third factor affecting sediments in Ranu Klakah is anthropogenic activity, characterised by the major elements Mn and P. Mn is likely to come from lake activities, such as fish feed waste, and can indicate redox (reduction-oxidation) processes under anoxic conditions at the bottom of the lake. P is a strong indicator of anthropogenic influence, especially from phosphate-rich fish feed or fertiliser runoff from surrounding areas (**Dunne et al., 2021**). A high P content also has the potential to trigger eutrophication, which is an increase in water fertility that leads to excessive algae growth. Thus, Mn and

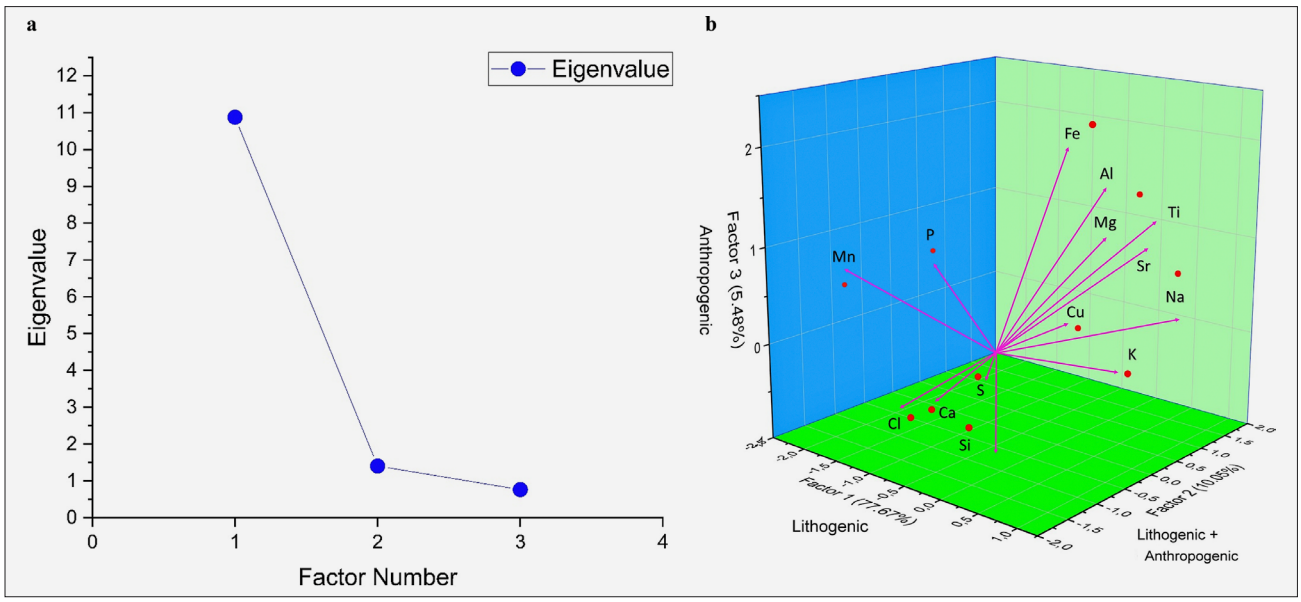

Figure 9. PCA plot of surface sediment of Ranu Klakah. a) scree plot of the characteristic roots (eigenvalues) and b) component plot in rotated space.

P reflect the direct impact of fish farm activities on sediment content in Ranu Klakah.

The XRD results of the two samples show the same mineral content, consisting of magnetite, albite, and illite. The presence of albite and illite minerals in the samples (see **Figure 7a-b**) reflects the influence of weathered volcanic material transported into the lake or the result of hydrothermal interaction between water and volcanic material at the bottom of the lake or surrounding area. Albite is a sodium-rich plagioclase feldspar that often forms through magmatic crystallisation or hydrothermal alteration in volcanic environments, so its presence is natural as Ranu Klakah is a maar lake that may have undergone chemical alteration in its environment (**Azer et al., 2019; Sun et al., 2020; Guo et al., 2021**). In addition, the presence of illite minerals also indicates hydrothermal activity that can trigger the formation of illite through interactions between volcanic host rocks and water-containing ions, especially potassium (K^+). The presence of illite in maar lake sediments suggests that the source of the sedimentary material is most likely from volcanic rocks around the lake, which underwent chemical changes before or during transport to the lake (**Bozkaya et al., 2016; Rodríguez-Salgado et al., 2021; Benson et al., 2023**). All identified minerals are common in volcanic environments (**Celik et al., 1999**).

5. Conclusions

In this study, it was concluded that the surface sediments in Ranu Klakah have a pseudo-single-domain magnetite mineral type, originating from the weathering of rocks transported from the surrounding area into the lake. Through rock magnetism and geochemical analyses, the minerals contained in the samples tend to be uniform, both those from the spring and those in the lake (even those close to the outlet). The variation in magnetic susceptibility values is due to differences in the concentration of magnetic minerals within the sediment rather than their type. So, it can be concluded that the diagenesis process has not occurred in Ranu Klakah sediments. Based on HCA and PCA analysis, anthropogenic factors have no significant contribution to the elemental content in Ranu Klakah.

Acknowledgements

This study was financially supported by the Ministry of Education, Culture, Research, and Technology 2024 to Satria Bijaksana, through a project entitled “Identification of lithogenic and anthropogenic components based on rock magnetism and geochemical properties of sediments in Ranu Klakah”. The grant number was LPPM1.PN-14-100-2024. We thank Dr. Prakash Kumar, Director of CSIR-National Geophysical Research Institute (CSIR-NGRI), Hyderabad, India, for his support in the collaboration between CSIR-NGRI and Institut Teknologi Bandung (ITB).

6. References

Asaah, A. N. E., Yokoyama, T., Aka, F. T., Iwamori, H., Kuritani, T., Usui, T., Gountie Dedzo, M., Tamen, J., Hassegawa, T., Fozing, E. M., Wirmvem, M. J., & Nche, A. L. (2020). Major/trace elements and Sr–Nd–Pb isotope systematics of lavas from lakes Barombi Mbo and Barombi Koto in the Kumba graben, Cameroon volcanic line: Constraints on petrogenesis. Journal of African Earth Sciences, 161. https://doi.org/10.1016/j.jafrearsci.2019.103675.

Azer, M. K., Gahlan, H. A., Asimow, P. D., & Al-Kahtany, K. M. (2019). The common origin and alteration history of the hypabyssal and volcanic phases of the Wadi Tarr albitite complex, southern Sinai, Egypt. Lithos, 324, 821–841. https://doi.org/10.1016/j.lithos.2018.12.015.

Barut, I. F., Ergin, M., Meriç, E., Avşar, N., Nazik, A., & Suner, F. (2018). Contribution of natural and anthropogenic effects in the Iznik Lake bottom sediment: Geochemical and microfauna assemblages’ evidence. Quaternary International, 486, 129–142. https://doi.org/10.1016/j.quaint.2017.10.026.

Benson, T. R., Coble, M. A., & Dilles, J. H. (2023). Hydrothermal enrichment of lithium in intracaldera illite-bearing claystones. Science Advances, 9(35), eadh8183. https://doi.org/10.1126/sciadv.adh8183.

Bijaksana, S., Megantara, G., Muchtar, C., Arandi, M. G. K., & Fajar, S. J. (2022). Identification of magnetic coercivity components in natural substances using Max Unmix web-application. Journal of Magnetism and Its Applications, 2(1), 1–4. https://doi.org/10.53533/jma.v2i1.17.

Bozkaya, Ö., Bozkaya, G., Uysal, I. T., & Banks, D. A. (2016). Illite occurrences related to volcanic-hosted hydrothermal mineralization in the Biga Peninsula, NW Turkey: Implications for the age and origin of fluids. Ore Geology Reviews, 76, 35–51. https://doi.org/10.1016/j.oregeorev.2016.01.001.

Carn, S. A. (2000). The Lamongan volcanic field, East Java, Indonesia: physical volcanology, historic activity and hazards. Journal of Volcanology and Geothermal Research, Vol. 95, 1-4, 81-108. https://doi.org/10.1016/S0377-0273(99)00114-6.

Celik, M., Karakaya, N., & Temel, A (1999). Clay Minerals in Hydrothermally Altered Volcanic Rocks, Eastern Pontides, Turkey. Clays and Clay Miner. 47, 708-717. https://doi.org/10.1346/CCMN.1999.0470604.

Day, R., Fuller, M., & Schmidt, V. A. (1977). Hysteresis Properties of Titanomagnetites: Grain-Size and Compositional Dependence. Physics of the Earth and Planetary Interiors, 13(4), 260-267. https://doi.org/10.1016/0031-9201(77)90108-X.

Dearing, J. A. (1994). Environmental magnetic susceptibility: using the Bartington MS2 system. Chi Pub.

Dunlop, D. J. (2002). Theory and application of the Day plot (Mrs/Ms versus Hcr/Hc) 1. Theoretical curves and tests using titanomagnetite data. Journal of Geophysical Research: Solid Earth, 107(B3), EPM-4. https://doi.org/10.1029/2001jb000486.

Dunne, A., Carvalho, S., Morán, X. A. G., Calleja, M. L., & Jones, B. (2021). Localized effects of offshore aquaculture

on water quality in a tropical sea. Marine pollution bulletin, 171, 112732. https://doi.org/10.1016/j.marpolbul.2021.112732.

Fagel, N., Israde-Alcántara, I., Safaierad, R., Rantala, M., Schmidt, S., Lepoint, G., Pellenard, P., Mattielli, N., & Metcalfe, S. (2024). Environmental significance of kaolinite variability over the last centuries in crater lake sediments from Central Mexico. Applied Clay Science, 247, 107211. https://doi.org/10.1016/j.clay.2023.107211.

Fajar, S. J., Suryanata, P. B., Wahidah, Hafidz, A., Bijaksana, S., Dahrin, D., & Iskandar, I. (2022). Geochemistry and rock magnetic analysis on surface sediment in Lampenisu River: a quest for Mg source to Lake Towuti, Indonesia. Rudarsko-geološko-naftni zbornik, 37(5), 149–157. https://doi.org/10.17794/rgn.2022.5.12.

Fu, H., Li, M., Bao, K., Zhang, Y., & Ouyang, T. (2024). Environment change recorded by lake sediment magnetism in the Songnen Plain, northeastern China. Science of the Total Environment, 919. https://doi.org/10.1016/j.scitotenv.2024.170938.

Graettinger, A. H. (2018). Trends in maar crater size and shape using the global Maar Volcano Location and Shape (MaarVLS) database. Journal of Volcanology and Geothermal Research, 357, 1–13. https://doi.org/10.1016/j.jvolgeores.2018.04.002.

Guo, P., Wen, H., Gibert, L., Jin, J., Wang, J., & Lei, H. (2021). Deposition and diagenesis of the Early Permian volcanic-related alkaline playa-lake dolomitic shales, NW Junggar Basin, NW China. Marine and Petroleum Geology, 123. https://doi.org/10.1016/j.marpetgeo.2020.104780.

Gurusinga, M. A., Ohba, T., Harijoko, A., & Hoshide, T. (2023). Characteristics of ash particles from the maar complex of Lamongan Volcanic Field (LVF), East Java, Indonesia: How textural features and magma composition control ash morphology. Volcanica, 6(2), 415–436. https://doi.org/10.30909/vol.06.02.415436.

Kaushik, S. J., Coves, D., Dutto, G., & Blanc, D. (2004). Almost total replacement of fish meal by plant protein sources in the diet of a marine teleost, the European seabass, Dicentrarchus labrax. Aquaculture, 230(1-4), 391-404. https://doi:10.1016/S0044-8486(03)00422-8.

Krishna, R., Wade, J., Jones, A. N., Lasithiotakis, M., Mummery, P. M., & Marsden, B. J. (2017). An understanding of lattice strain, defects and disorder in nuclear graphite. Carbon, 124, 314-333. https://doi.org/10.1016/j.carbon.2017.08.070.

Lorenz, V. (1986). On the growth of maars and diatremes and its relevance to the formation of tuff rings. Bulletin of Volcanology, 48, 265-274. https://doi.org/10.1007/BF01081755.

Noya, Y., Bijaksana, S., Fajar, S. J., Suryanata, P. B., Harlianti, U., Ibrahim, K., Suandayani, N. K. T., Multi, W., & Bahri, S. (2024). Magnetic susceptibility in the assessment of toxic heavy metal elements in the surface sediments of Inner Ambon Bay, Maluku province, Indonesia. Heliyon, 10(6). https://doi.org/10.1016/j.heliyon.2024.e27497.

Panagos, P., Ballabio, C., Lugato, E., Jones, A., Borrelli, P., Scarpa, S., Orgiazzi, A., & Montanarella, L. (2018). Potential sources of anthropogenic copper inputs to European agricultural soils. Sustainability, 10(7), 2380. https://doi.org/10.3390/su10072380

Paterson, G. A., Zhao, X., Jackson, M., & Heslop, D. (2018). Measuring, Processing, and Analyzing Hysteresis Data. Geochemistry, Geophysics, Geosystems, 19(7), 1925–1945. https://doi.org/10.1029/2018GC007620.

Rodríguez-Salgado, P., Oms, O., Ibáñez-Insa, J., Anadón, P., Gómez de Soler, B., Campeny, G., & Agustí, J. (2021). Mineralogical proxies of a Pliocene maar lake recording changes in precipitation at the Camp dels Ninots (Pliocene, NE Iberia). Sedimentary Geology, 418. https://doi.org/10.1016/j.sedgeo.2021.105910.

Sabatier, P., Moernaut, J., Bertrand, S., Van Daele, M., Kremer, K., Chaumillon, E., & Arnaud, F. (2022). A Review of Event Deposits in Lake Sediments. Quaternary, 5(3), 34. https://doi.org/10.3390/quat5030034.

Siaka, M., Owens, C. M., & Birch, G. F. (1998). Evaluation of some digestion methods for the determination of heavy metals in sediment samples by flame-aas. Analytical Letters, 31(4), 703–718. https://doi.org/10.1080/00032719808001873.

Storebakken, T., Shearer, K. D., & Roem, A. J. (1998). Availability of protein, phosphorus and other elements in fish meal, soy-protein concentrate and phytase-treated soy-protein-concentrate-based diets to Atlantic salmon, Salmo salar. Aquaculture, 161(1-4), 365-379. https://doi.org/10.1016/S0044-8486(03)00422-8.

Suandayani, N. K. T., Harlianti, U., Fajar, S. J., Suryanata, P. B., Ibrahim, K., Bijaksana, S., Dahrin, D., & Iskandar, I. (2023). Religious activities and their impacts on the surface sediments of two lakes in Bali, Indonesia: A case study from Lake Buyan and Lake Tamblingan. Elementa, 11(1), 105–122. https://doi.org/10.1525/elementa.2022.00140.

Sudarningsih, S., Bijaksana, S., Ramdani, R., Hafidz, A., Pratama, A., Widodo, W., Iskandar, I., Dahrin, D., Fajar, S. J., & Santoso, N. A. (2017). Variations in the concentration of magnetic minerals and heavy metals in suspended sediments from Citarum river and its tributaries, West Java, Indonesia. Geosciences (Switzerland), 7(3), 66. https://doi.org/10.3390/geosciences7030066.

Sun, Z., Wang, J., Wang, Y., Long, L., Luo, Z., Deng, X., Hu, Q., & Wang, M. (2020). Sodium-rich volcanic rocks and their relationships with iron deposits in the Aqishan–Yamansu belt of Eastern Tianshan, NW China. Geoscience Frontiers, 11(2), 697–713. https://doi.org/10.1016/j.gsf.2019.06.011.

Tamuntuan, G., Bijaksana, S., Gaffar, E., Russell, J., Safiuddin, L. O., & Huliselan, E. (2010). The magnetic properties of Indonesian Lake Sediment: A case study of a tectonic lake in South Sulawesi and maar lakes in East Java. ITB Journal of Science A, 42, 31-48. https://doi.org/10.5614/itbj.sci.2010.42.1.4.

Tao, H., Hao, L., Li, S., Wu, T., Qin, Z., & Qiu, J. (2021). Geochemistry and Petrography of the Sediments from the Marginal Areas of Qinghai Lake, Northern Tibet Plateau, China: Implications for Weathering and Provenance. Frontiers in Earth Science, 9. https://doi.org/10.3389/feart.2021.725553.

Tauxe, L., Bertram, H. N., & Seberino, C. (2002). Physical interpretation of hysteresis loops: Micromagnetic modeling of fine particle magnetite. Geochemistry, Geophysics, Geosystems, 3(10), 1-22. https://doi.org/10.1029/2001GC000241.

Tekin-Özan, S., Tunç, M., & Bakioğlu-Acar, B. (2024). Evaluation of some heavy metals and selenium pollution in Karataş Lake (Burdur/Türkiye) using various pollution indices and statistical analysis. Marine Pollution Bulletin, 199. https://doi.org/10.1016/j.marpolbul.2023.115927.

Topaldemir, H., Taş, B., Yüksel, B., & Ustaoğlu, F. (2023). Potentially hazardous elements in sediments and Ceratophyllum demersum: an ecotoxicological risk assessment in Miliç Wetland, Samsun, Türkiye. Environmental Science and Pollution Research, 30(10), 26397–26416. https://doi.org/10.1007/s11356-022-23937-2

Varol, M. (2019). Impacts of cage fish farms in a large reservoir on water and sediment chemistry. Environmental Pollution, 252, 1448-1454. https://doi.org/10.1016/j.envpol.2019.06.090.

Venkateshwarlu, M., & Satyakumar, A. V. (2024). Paleomagnetism of mafic dykes in South Rewa Basin, India: Constraints to extension of Deccan volcanism. Geosystems and Geoenvironment, 3(3). https://doi.org/10.1016/j.geogeo.2024.100292.

Vigliotti, L., Bilardello, D., Winkler, A., & Del Carlo, P. (2022). Rock magnetic fingerprint of Mt Etna volcanic ash. Geophysical Journal International, 231(2), 749–769. https://doi.org/10.1093/gji/ggac213.

Vogel, A., Diplas, S., Durant, A. J., Azar, A. S., Sunding, M. F., Rose, W. I., Sytchkova, A., Bonadonna, C., Krüger K., & Stohl, A. (2017). Reference data set of volcanic ash physicochemical and optical properties. Journal of Geophysical Research: Atmospheres, 122(17), 9485-9514. https://doi.org/10.1002/2016JD026328.

Volosín, S.M., & Risso, C. (2019). El Pozo Volcanic Complex: Evolution of a group of maars, central Mendoza province, Argentina. Journal of Volcanology and Geothermal Research, 371, 177–191. https://doi.org/10.1016/j.jvolgeores.2019.01.005.

Wang, Y., Huang, Q., Lemckert, C., & Ma, Y. (2017). Laboratory and field magnetic evaluation of the heavy metal contamination on Shilaoren Beach, China. Marine Pollution Bulletin, 117(1–2), 291–301. https://doi.org/10.1016/j.marpolbul.2017.01.080.

Yüksel, B., Ustaoğlu, F., Tokatli, C., & Islam, M. S. (2022). Ecotoxicological risk assessment for sediments of Çavuşlu stream in Giresun, Turkey: association between garbage disposal facility and metallic accumulation. Environmental Science and Pollution Research, 29(12), 17223–17240. https://doi.org/10.1007/s11356-021-17023-2.

Yunginger, R., Bijaksana, S., Dahrin, D., Zulaikah, S., Hafidz, A., Kirana, K. H., Sudarningsih, S., Mariyanto, M., & Fajar, S. J. (2018). Lithogenic and anthropogenic components in surface sediments from lake Limboto as shown by magnetic mineral characteristics, trace metals, and REE geochemistry. Geosciences, 8(4), 116. https://doi.org/10.3390/geosciences8040116.

SAŽETAK

Magnetizam stijena i geokemijske analize površinskih sedimenata kraterskoga jezera: studija slučaja Ranu Klakah, Istočna Java, Indonezija

Ranu Klakah kratersko je jezero koje je dio monogenetskoga vulkanskog polja Lamongan (LMVF), Istočna Java, Indonezija, koje ima zatvoreni hidrološki sustav. Cilj je ove studije ustanoviti karakteristike površinskih sedimenata u Ranu Klakahu korištenjem magnetizma stijena i geokemijskih analiza. Ispitivanja su provedena na 16 uzoraka površinskih sedimenata u jezeru i iz izvora oko jezera. Rezultati analize magnetizma stijena u površinskim sedimentima Ranu Klakaha pokazali su prisutnost minerala magnetita i titanomagnetita. Navedeni rezultati potvrđeni su rendgenskom difrakcijom na prahu (XRD analiza), gdje je zabilježena pojava magnetita, albita i ilita u promatranim sedimentima. Korištenjem rezultata obiju metoda zaključeno je da površinski sedimenti u Ranu Klakahu imaju pseudojednodomenske magnetitne minerale koji su nastali kao posljedica trošenja stijena oko jezera te da nije dolazilo do dijageneze površinskih sedimenata u jezeru, što se pretpostavlja zbog nedostatka rezultata koji mogu upućivati na mineralne promjene u testiranim uzorcima.

Ključne riječi:
kratersko jezero, monogenetsko vulkansko polje Lamongan, magnetizam stijena, geokemijske značajke, Istočna Java

Author's contribution

Fathia Matondang (BEng, geophysical engineer with expertise in geophysical exploration) performed and conceived the study, participated in the field survey, prepared the sediment samples, measured and analyzed rock magnetism and geochemistry data, and composed the original drafting. **Satria Bijaksana** (PhD, Rock magnetism Professor) performed and conceived the study, interpreted rock magnetism data, edited drafts, and held funding acquisition, and supervision. **Ulvienin Harlianti** (MEng, geophysical engineer with expertise in rock magnetism and geochemistry for environmental purposes) conceived the study, participated in the field survey, provided the data interpretation, and edited the draft. **Ni Komang Tri Suandayani** (PhD, Geophysical lecturer with expertise in rock magnetism for environmental purposes) prepared the sediment samples. **Yohansli Noya** (MEng, geophysical engineer with expertise in geophysical exploration for environmental purposes) performed HCA and PCA analysis. **Putu Billy Suryanata** (PhD, Geophysical lecturer with expertise in rock magnetism for volcano field) participated in the field survey and project administration. **Khalil Ibrahim** (MEng, geophysical engineer with expertise in geophysical exploration) participated in the field survey and edited the draft. **Thomas Andre Maris Widagdo** (MEng, geophysical engineer with expertise in geophysical exploration) participated in the field survey. **Mamilla Venkateshwarlu** (PhD, researcher with expertise in palaeomagnetism) measured rock magnetism: hysteresis loops, thermomagnetic, and isothermal remanent magnetization. **Animireddi Venkata Satyakumar** (PhD, researcher with expertise in palaeomagnetism) measured rock magnetism: hysteresis loops, thermomagnetic, and isothermal remanent magnetization.
All authors have read and agreed to the published version of the manuscript.